TÜBİTAK

Turkish Journal of Earth Sciences

http://journals.tubitak.gov.tr/earth/

Research Article

Turkish J Earth Sci
(2015) 24: 276-288

doi:10.3906/yer-1410-21

Petrography and geochemistry of the Kamlial Formation, southwestern Kohat plateau, Pakistan: implications for paleoclimate of the Western Himalayas

Kafayat ULLAH[1], Mohammad ARIF[2,3]*, Muhammad TAHIR SHAH[4]

[1]Regional Exploration Office, Pakistan Atomic Energy Commission, Peshawar, Pakistan
[2]Department of Geology, University of Peshawar, Peshawar, Pakistan
[3]Department of Earth Sciences, COMSATS Institute of Information Technology, Abbottabad, Pakistan
[4]National Center of Excellence in Geology, University of Peshawar, Peshawar, Pakistan

Received: 29.10.2014 • **Accepted/Published Online:** 04.03.2015 • **Printed:** 29.05.2015

Abstract: The Middle to Late Miocene Kamlial Formation that largely consists of sandstone and interbedded clay/mudstone sequences is exposed in the southwestern part of the Kohat plateau, which constitutes the westernmost extension of the Himalayan Foreland Basin. Whereas the sandstone is gray to brownish gray, fine- to medium-grained, and mostly thick-bedded, the interbedded clay/mudstone sequence is brownish gray to maroon red and occurs as continuous beds as well as lenses. Some mudstone/clay beds are bioturbated and seem to be pedogenic surfaces. Results of geochemical investigation of fresh (unaltered) representative sandstone and mudstone samples from three different sections of the formation in the southwestern Kohat plateau are presented and discussed. The average chemical index of alteration (CIA) values of both the sandstone (70–86) and mudstone (71–85) suggest moderate to slightly intense weathering in the source area. However, the high CIA values may also be due to the presence of abundant sedimentary rock fragments, which occur in the studied sandstone, rather than a result of severe weathering. Furthermore, the possibility of intensive chemical weathering in the Himalayas orogenic belt is highly unlikely, as it requires tectonic quiescence for a long period, higher temperature, and humidity. Accordingly, the range of the index of chemical variability values (0.6–2.1) of mudstone and low contents of Rb and Cs in both the mudstone and sandstone indicate somewhat moderate weathering. Furthermore, the Th/U and Rb/Sr ratios of the Kamlial Formation are lower than the corresponding average values for the upper continental crust and post-Archean average Australian shale, which shows that these sediments are first-cycled in origin. However, the Zr/Sc ratio indicates minor contributions from recycled sedimentary sources. The values of authigenic U and the U/Th, V/Cr, Cu/Zn, and Ni/Co ratios all suggest that the Kamlial sediments were deposited under oxidizing conditions.

Key words: Miocene, sandstones, mudstones, geochemistry, weathering, recycling, paleoenvironment

1. Introduction

The Himalayan Foreland Basin is one of the largest and dynamic terrestrial basins. It is divided into a number of subbasins separated by several pre-Tertiary basement highs/lineaments (Raiverman, 2002). In Pakistan, two main sedimentary basins, namely the Indus and the Balochistan basins, have been identified. The former contains excellent exposures of the Middle to Late Miocene Kamlial Formation in the Kohat and Potwar plateaus (Kadri, 1995). The sedimentary sequence of the Kamlial Formation preserves the record of the tectonic processes and climatic conditions of the Western Himalayan orogeny and sedimentation pattern and drainage organization at the subbasin level for that time period (Figure 1; Kumar et al., 2003). The present study focuses on three sections of the Kamlial Formation exposed in the southwestern part of the Kohat plateau, which constitutes the westernmost part of the Himalayan Foreland Basin and comprises regional scale folds and thrust faults. Important folds in this region include the Karak anticline, Nari Panoos syncline, Chashmai anticline, Banda Assar syncline, and Bahadar Khel anticline. The last three structures, i.e. the Chashmai anticline (33°06′34″N, 70°47′77″E), Banda Assar syncline (33°07′52″N, 70°55′88″E), and Bahadar Khel anticline (33°09′79″N, 70°57′64″E), were selected for the present investigation (Figure 2).

2. Major structures of the Western Himalayas

Along its strike, the Himalayan orogen is subdivided into Western, Central, and Eastern segments. The last mentioned segment extends into Pakistan (Yin, 2006). The Himalayan tectonic evolution consists of two stages:

* Correspondence: arif_pkpk@yahoo.com

the Eo-Himalayan event (Middle Eocene to Oligocene, i.e. 45–25 Ma) and the Neo-Himalayan event (since the Early Miocene) (Hodges, 2000).

The Himalayan mountain belt consists of a series of thrust sheets, whose southward propagation began soon after the India-Eurasia collision in the Eocene (Figure 1; Searle et al., 1997). These include the Indus Suture Zone (ISZ), which separates the Indian and Asian crusts; the South Tibetan Detachment Zone (STDZ) that demarcates the Tibetan Himalaya Zone (THZ) from the metamorphosed Indian plate rocks constituting the Greater Himalayan Crystalline Complex (GHC); and the Main Central Thrust (MCT) that marks the boundary between the GHC and the mostly Precambrian- to Paleozoic-aged Lesser Himalaya (Searle et al., 1997; Vance and Harris, 1999). The last phase of peak metamorphism, circa 20 Ma, is associated with movement along the MCT and normal faulting at the base of the THZ along the STDZ (Metcalfe, 1993). Continued convergence of India with Eurasia resulted in southward propagation of the thrust belt. As a result, the Main Boundary Thrust (MBT), which was active in the Middle-Late Miocene (~10 Ma; Meigs et al., 1995) or Pliocene time (DeCelles et al., 1998), placed the LHZ over the Sub-Himalaya. However, there is another model, i.e. the steady-state model, whereby the MBT and MCT are thought to be contemporaneous and still active (Seeber et al., 1981). This view is supported by several lines of geological and geomorphological evidence for ongoing tectonic activity along both the MCT (Seeber and Gornitz, 1983) and the MBT (Valdiya, 1992).

3. Sampling and geochemical analyses

Sixteen unweathered sandstone and mudstone samples representing variation in color and texture were selected from three different sections of the Kamlial Formation in the Kohat Plateau. Six each of the selected samples represent the Banda Assar syncline and Bahadar Khel anticline, symbolized as A and B, respectively, while the remaining four, coded as C, are from the Chashmai anticline. The sandstone is grey to brownish gray, fine- to medium-grained, and mostly thick-bedded. The interbedded clay/mudstone sequence is brownish-gray to maroon red and occurs as continuous beds as well as lenses pinching out at short distances (≥20 m). Some mudstone/clay beds are bioturbated and seem to be pedogenic surfaces. At places, the mudstone is multistoried, containing abundant vertical burrows and caliche horizon toward the top of an individual story.

The analytical work included major element analyses with atomic absorption spectrometer (AAS)/UV-visible spectrophotometer as well as X-ray fluorescence (XRF), spectrometer, and trace element analyses by XRF spectrometer.

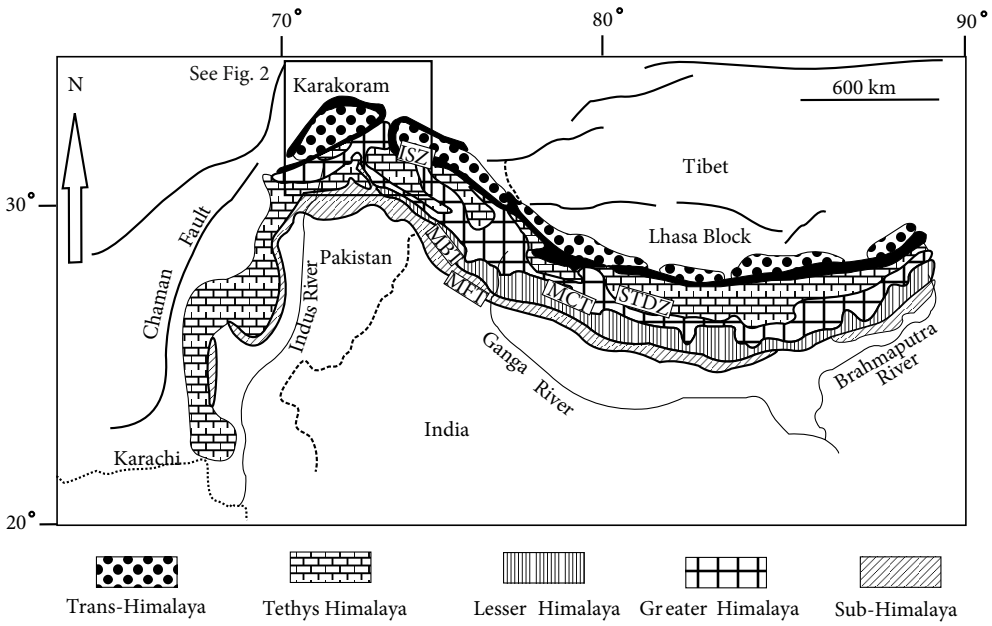

Figure 1. Location map of the Himalayan Range (modified from Critelli and Garzanti, 1994; Najman, 2006). The thick continuous lines indicate faults and suture zones, and the major ones among them are labeled as follows: ISZ = Indus Suture Zone, STDZ = South Tibetan Detachment Zone, MCT = Main Central Thrust, MBT = Main Boundary Thrust, MFT = Main Frontal Thrust. The thinner lines show major rivers and are named accordingly. The dashed line marks the international boundary between Pakistan and India.

Major elements were measured from the fusion disks. The corresponding Geological Survey of Japan standard samples were run with every batch of ten samples using the RIGAKU XRF-3370E spectrometer at the Geoscience Advanced Research Laboratories, Geological Survey of Pakistan, Islamabad. The results of analyses were then compared with the recommended values of USGS standard reference samples (Govindaraju, 1989). The detection limits of XRF for major elements (wt.%) are as follows: SiO_2 (0.27), TiO_2 (0.014), Al_2O_3 (0.13), Fe_2O_3 (0.08), MnO (0.005), MgO (0.03), CaO (0.09), Na_2O (0.02), K_2O (0.03), and P_2O_5 (0.03).

The trace elements analyses were performed on pressed powder pellets using a Philips PW 1480 XRF at the National Center of Excellence in Geology (NCEG), University of Peshawar, Pakistan. To avoid particle size effects, the very finely powdered samples were homogenized with a fusion material (wax). Furthermore, major elements were also analyzed by AAS/UV spectrophotometer at the NCEG Geochemistry Laboratory. All of the analyses were in good agreement in replicate.

The level of precision for major elements is normally better than 6% while the precision for most of the trace elements is better than 5%, the exception being Yb, whose precision is normally better than 7%. Total iron is reported as Fe_2O_3 (Cullers, 2000). Methods of chemical analysis, descriptions of sample sets, and estimates of analytical error are as given in detail by Connor (1990).

4. Results and discussion

4.1. Geochemistry and chemical classification of the Kamlial sandstone

The Kamlial sandstone of the Himalayan Foreland Basin from the Kohat plateau has been classified as feldspathic arenite and lithic arenite on the basis of petrography (Ullah et al., 2006). Accordingly, its chemical composition is well within the range of the mean chemical composition of lithic arenites and feldspathic arenites (Tables 1 and 2). The only components that depart significantly from the range of the mentioned two classes are SiO_2 and CaO; the former is low while the latter is high to very high in the studied sandstone from the southwestern Kohat plateau (Table 2). The very high amount of CaO in the studied sandstone (7.5%–20.4%) is because of the presence of secondary $CaCO_3$. The mean contents of CaO in lithic and feldspathic arenites are 6.2% and 2.0%, respectively. Furthermore, the relatively high loss on ignition (LOI) values of the studied sandstone and mudstone samples (Table 1) reflect the presence of variable amounts of carbonate and hydrous phases (cf. Gu et al., 1997).

The medium- to fine-grained sandstone samples of the study area are well classified by the scatter-plots based on log (SiO_2/Al_2O_3), log (Na_2O/K_2O), and log (Fe_2O_3/K_2O) (Figure 3). On the log (SiO_2/Al_2O_3) versus log (Na_2O/K_2O) scattergram, the studied sandstones are predominantly classified as litharenite; however, a few of the samples do fall in the graywacke field, and only one plots as arkose (Figure 3a). On the log (SiO_2/Al_2O_3) versus log (Fe_2O_3/K_2O) scattergram, however, the same samples dominantly fall into the Fe-sand field, although a few of them plot in the Fe-shale and wacke fields (Figure 3b). The shift of sandstone to various fields is due to a wide range in the variation of the relative proportion of matrix, feldspar, and lithic components (see also Lindsey et al., 2003). Besides, chemical variation, particularly in terms of SiO_2/Al_2O_3 and (Na_2O/K_2O), may also result from varying degrees of weathering of initially Na_2O-rich (plagioclase) rock either at the source and/or during transit to the depositional basin. As care was taken to avoid collecting weathered samples, the latter explanation is not applicable to the data from the present study.

4.2. Chemical index of alteration and chemical index of weathering

Major element chemistry can best be employed for determining the extent of weathering at the source area once the general tectonic setting is established by other means. Both the chemical index of alteration (CIA) [$\{A1_2O_3 / (AI_2O_3 + CaO^* + K_2O + Na_2O)\} \times 100$] and chemical index of weathering (CIW) [$\{A1_2O_3 / (AI_2O_3 + CaO^* + Na_2O)\} \times 100$] are based on major element data. CaO* is the amount of CaO incorporated in the silicate fraction of the rock and is presented in molar proportions to emphasize mineralogical relationships (Nesbitt and Young, 1982). The highly variable values of CaO in the studied samples (Tables 1 and 2) are because of the presence of secondary $CaCO_3$. Fedo et al. (1995) proposed a correction assuming the rocks' CO_2 contents to be equivalent to CaO contributions from nonsilicate minerals. As the studied samples were not analyzed for CO_2, distinction between CaO contributions from carbonates and silicates (feldspars) is not readily possible. Although rare in the Kamlial samples, plagioclase occurring as one of the major constituents is the chief source of Ca in many sandstones. Similarly, sphene could be another important source of Ca as it occurs more or less commonly, albeit as an accessory mineral in sandstones. However, grains of sphene were not observed at all in the investigated samples. Hence, it may be presumed that molar CaO* contributions from silicates in the calculation are negligible. That is why CaO* is deliberately omitted from the CIA and CIW calculations and the corresponding indices adopted in this study are designated as CIA' and CIW', respectively, which are close and reasonable approximations of the former (Cullers, 2000).

Low CIA/CIW values indicate negligible alteration/weathering, whereas moderate or high CIA/CIW values are

Table 1. Bulk chemical analyses of the Kamlial sandstone and mudstone samples from southwestern Kohat plateau, NW Pakistan. The letter in the sample numbers refers to locality: C for Chashmai anticline, A for Banda Assar syncline, and B for Bahadar Khel anticline. CIA = Chemical index of alteration, CIW = chemical index of weathering, ICV = index of compositional variability.

Rock type	Sandstone											Mudstone				
Sample #	C-1	C-4	C-10	A-40	A-42	A-44	A-52	B-88	B-95	B-97	B-100	C-8	A-41	A-43	B-90	B-98
SiO_2	48.94	57.21	56.23	51.25	52.24	46.87	49.81	63.43	47.41	56.10	49.68	50.33	39.68	31.58	47.72	40.47
Al_2O_3	8.35	9.14	10.30	14.51	7.45	23.33	6.70	6.88	6.51	8.88	6.06	12.93	22.84	10.58	7.52	9.94
Fe_2O_3	3.75	4.21	4.47	3.07	2.52	4.48	2.74	4.76	4.42	3.73	2.83	6.80	6.67	4.37	6.60	5.24
MgO	3.48	2.07	3.18	1.49	0.94	2.64	0.98	3.52	1.97	1.96	1.59	2.78	2.96	2.36	5.12	3.41
CaO	16.15	12.16	11.01	15.46	20.41	9.10	18.50	7.48	19.26	10.00	19.81	8.00	9.63	27.43	11.53	18.61
Na_2O	1.01	0.51	0.73	1.18	1.12	1.41	1.06	0.87	0.76	0.94	0.81	1.09	1.07	0.99	0.54	0.96
K_2O	1.50	1.49	1.66	1.34	1.16	1.38	1.07	1.34	1.15	1.18	1.09	2.07	2.24	1.69	1.99	1.46
TiO_2	0.32	0.82	0.70	0.64	0.60	0.93	0.54	0.70	0.84	0.86	0.57	0.97	1.03	0.52	1.51	1.16
P_2O_5	0.11	0.09	0.13	0.06	0.07	0.15	0.06	0.11	0.11	0.09	0.07	0.10	0.10	0.10	0.09	0.09
MnO	0.18	0.11	0.15	0.13	0.19	0.00	0.09	0.09	0.23	0.12	0.19	0.11	0.13	0.13	0.10	0.12
LOI	16.22	12.18	11.40	10.94	13.26	9.78	16.79	10.72	17.47	16.14	17.57	14.61	13.59	20.35	16.78	18.48
Total	100.02	99.99	99.96	100.08	99.95	100.06	98.33	99.91	100.12	100.00	100.26	99.78	99.96	100.09	99.51	99.95
CIA	71.72	78.80	77.44	81.06	70.60	85.93	69.75	70.44	72.34	75.86	70.74	76.24	84.49	75.35	71.16	75.85
CIW	0.89	0.95	0.93	0.92	0.87	0.94	0.86	0.89	0.90	0.90	0.88	0.92	0.96	0.91	0.93	0.91
ICV	1.23	1.01	1.06	0.54	0.88	0.46	0.97	1.64	1.44	0.99	1.17	1.07	0.62	0.95	2.11	1.24
Trace elements (ppm)																
Sc	14	12	13	10	12	12	15	12	19	13	16	12	13	18	19	15
V	51	52	58	33	33	64	29	54	58	65	36	81	97	59	110	71
Cr	162	285	86	230	161	224	59	191	175	409	183	92	122	56	97	287
Co	43	51	48	45	22	44	39	44	30	41	43	17	21	13	19	22
Ni	112	114	40	34	27	31	35	222	41	92	78	68	101	25	79	170
Cu	6	17	12	10	5	11	14	5	13	7	3	33	33	20	37	17
Zn	29	32	40	26	23	39	26	41	34	33	25	69	77	46	70	50

Table 1. (Continued).

Rock type	Sandstone											Mudstone				
Ga	6	7	8	7	6	10	5	8	8	7	5	13	14	8	12	9
Rb	45	52	56	59	46	64	53	58	49	48	41	99	117	72	82	61
Sr	168	134	239	219	207	221	176	135	190	127	147	238	134	146	345	140
Y	13	13	17	14	18	18	10	12	21	15	10	21	17	19	20	17
Zr	81	104	102	95	97	121	74	91	96	120	105	178	118	89	121	163
Nb	6	7	6	5	6	8	5	7	6	7	6	12	12	8	10	10
Ag	4	5	6	5	4	7	5	3	7	7	4	9	2	4	6	5
Cd	2	3	3	4	3	4	4	0	2	5	4	3	3	1	5	3
Sn	1	6	4	7	4	6	5	2	4	4	3	3	4	1	4	3
Sb	6	0	1	5	9	0	1	0	6	0	13	2	0	6	3	4
Cs	0	0	0	3	0	0	14	0	0	0	6	16	26	16	12	5
Ba	132	165	188	232	156	222	154	176	186	173	138	134	186	205	173	172
La	30	28	17	23	20	23	22	28	28	26	25	37	35	34	27	31
Ce	37	56	20	38	27	42	8	23	54	13	39	56	52	32	12	53
Nd	19	25	17	30	21	33	16	27	31	26	21	28	33	28	32	48
Sm	0	11	0	0	0	0	0	0	0	0	0	7	0	0	6	0
Yb	4	0	0	1	0	0	1	2	0	13	1	5	6	0	0	0
Hf	5	4	6	1	1	5	1	6	2	3	2	11	6	7	4	4
Ta	1	0	4	0	0	0	0	0	3	1	3	0	0	0	1	0
W	548	480	499	362	29	331	310	264	183	297	311	41	39	28	18	104
Pb	7	9	10	11	10	11	11	6	11	8	6	18	17	16	18	13
Th	5	7	6	5	6	8	6	5	6	6	6	12	10	9	10	9
U	1	3	4	3	3	3	2	3	5	4	14	5	4	3	6	4

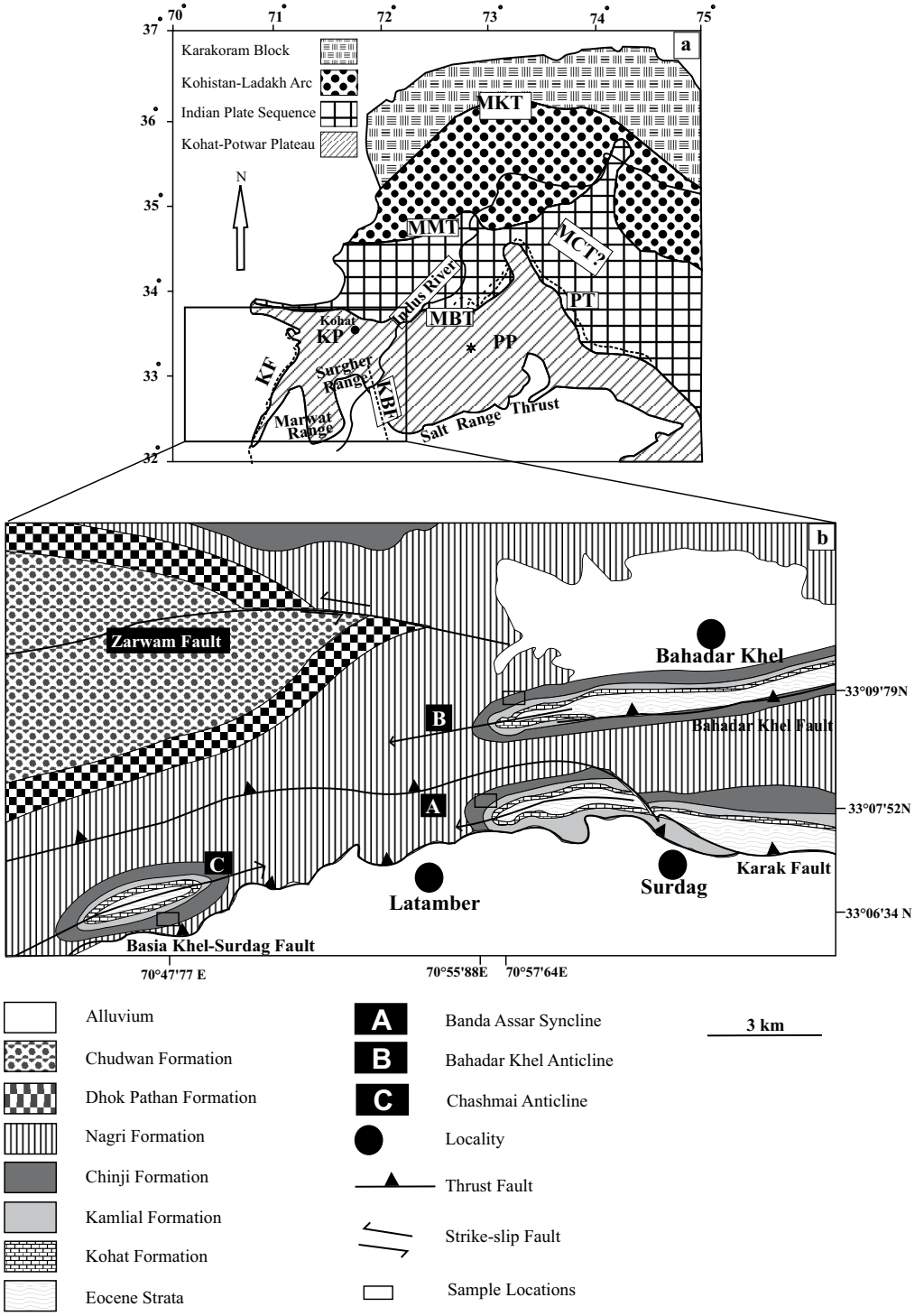

Figure 2. (a) Regional tectonic map of northern Pakistan (modified after Kazmi and Rana, 1982): MKT = Main Karakoram Thrust, MMT = Main Mantle Thrust, PT = Panjal Thrust, MBT = Main Boundary Thrust, KP = Kohat Plateau, PP = Potwar Plateau, KF = Kurram Fault, KBF = Kalabagh Fault. The star marks location of the type section from which various microfossils indicating the age of the Kamlial Formation are reported (cf. Shah, 2009). **(b)** Geological map of a part of the Kohat plateau (after Meissner et al., 1974; Ahmad et al., 2001). The small open rectangles show locations of the studied samples from Banda Assar syncline (A), Bahadar Khel anticline (B), and Chashmai anticline (C). The arrows indicate plunging directions of the three structures.

Figure 2. (c) Panoramic view of the Bahadar Khel anticline (looking north). The white lines mark contacts between the three studied formations, i.e. Kamlial Formation (oldest), Chinji Formation, and Nagri Formation (youngest).

correlated with the removal of mobile cations (e.g., Ca^{++}, Na^{+}, and K^{+}) relative to the less mobile residual constituents (Al^{+++} and Ti^{+4}) (Nesbitt and Young, 1982). A CIA value of about 50 generally indicates first-cycle sediments; the CIA tends to increase as chemical weathering intensifies (Nesbitt and Young, 1982). The CIA value of the main rock-forming minerals (quartz, plagioclase, alkali feldspars, pyroxene, and olivine) is ≤55, whereas clay minerals yield higher CIA values that are usually ≥75. High values of the index, i.e. >90%, indicate extensive conversion of feldspar to clay and hence intense alteration/weathering. In general, the CIA values in Phanerozoic shales range from 70 to 75, reflecting muscovite, illite, and smectite compositions and a moderately altered/weathered source (Nesbitt and Young, 1982). The CIA value for post-Archean Australian shale (PAAS) is 69 (Nesbitt et al., 1980).

Averaging 75, the CIA' values for the studied sandstone range from 70 to 86 (Table 1). The CIA' values of five of the samples are greater than 75, which suggests the presence of appreciable amounts of feldspar in sandstone and reflects moderate weathering in the source areas. The presence of sedimentary rock fragments in the Kamlial sandstones (Ullah et al., 2006) reveals that the high CIA' values were produced partly by recycling of older sediments rather than solely by intense weathering, as also suggested by Lee (2002).

The CIA' values of the studied mudstone samples (averaging 77; Table 1) are higher than the CIA value of PAAS, suggesting relatively intense source-area weathering. However, the presence of abundant sedimentary rock fragments in the associated sandstones (Ullah et al., 2006) indicates that the high CIA values could be in part because of older sediments (recycling) rather than just severe weathering (see also Lee, 2002).

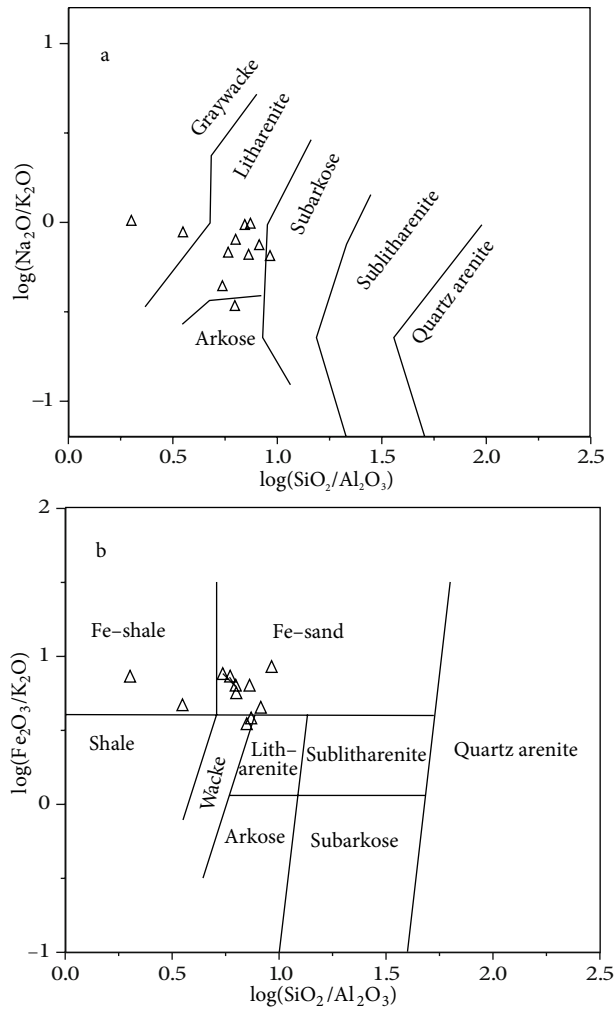

Figure 3. Whole-rock data on Kamlial sandstone from southwestern Kohat plateau plotted as triangles on the geochemical classification diagrams of (A) Herron (1988) and (B) Pettijohn et al. (1987).

4.3. Index of compositional variability

Cox et al. (1995) proposed a measure of compositional variability, known as the index of compositional variability (ICV) [= (CaO + K_2O + Na_2O + Fe_2O_3(t) + MgO + MnO + TiO_2) / $A1_2O_3$]. Here, Fe_2O_3(t) is the amount of total iron and CaO includes Ca from all sources. Unlike CIA and CIW, the ICV is based on weight percent oxides rather than moles. The value of ICV decreases with increasing degree of weathering. The ICV values of some of the relatively common minerals are: ~10–100 (pyroxene and amphibole), ~8 (biotite), ~0.8–1 (alkali feldspar), ~0.6 (plagioclase), ~0.3 (muscovite and illite), 0.14–0.3 (montmorillonite), and ~0.03–0.05 (kaolinite) (Cox et al., 1995). Median ICV values (<0.6) for mudrocks fall within the range of clay minerals, whereas ICV values of >0.7 indicate the presence of a large nonclay fraction. The

overall range of the ICV values for the studied Kamlial mudstone (0.6–2.1; Table 1) indicates somewhat moderate weathering in the source area. This interpretation is supported by the presence of substantial feldspar in the associated sandstones (Ullah et al., 2006).

The ratio of K_2O/Al_2O_3 can also be used as an indicator of the original composition of ancient mudrocks. The K_2O/Al_2O_3 ratios for feldspars (e.g., alkali feldspars = 0.4–1.0) are markedly different from those of clay minerals (~0.3 for illite and nearly 0 for other clay minerals) (Cox et al., 1995). The K_2O/Al_2O_3 ratios of the investigated mudstones from the Kamlial Formation are less than 0.3 (Table 3), suggesting the preponderance of clay minerals relative to other minerals in the original mudstone (Cox et al., 1995). As concluded above, the high ICV values of the Kamlial mudstone indicate dominance of nonclay silicate material such as feldspar, whereas the low average K_2O/Al_2O_3 ratio suggests just the opposite (Table 3). Although K has a high aqueous solubility, the chemical stability of illite tends to preserve it (Lee and Ko, 1997). The presence of illite in mudstone may indicate recycling of older sediments (Potter et al., 1980).

Moderate weathering conditions in the source area for the Kamlial Formation is also in agreement with compositions indicated by the presence of unstable lithic fragments in the interbedded sandstones (Ullah et al., 2006). It should also be noted that high ICV values of mudrocks are probably due to the presence of calcite cement and high Fe_2O_3 content (indicated by red or maroon color of the mudstone; Table 1), which may be the result of chemical weathering during pedogenesis within the depositional basin. High ICV values of mudrocks show the dominance of first-cycle detritus, supporting the results of sandstone petrological studies (Ullah et al., 2006).

4.4. Trace elements and degree of weathering and conditions of deposition

4.4.1. Large ion lithophile elements

Large ion lithophile elements such as Rb, Sr, Ba, Th, U, and Cs behave much like the related major elements during weathering processes. For example, whereas Rb and Cs are generally incorporated into clays, as is also K_2O, Sr tends to leach out during chemical weathering, as do also CaO and Na_2O (Nesbitt et al., 1980). The amounts of Rb and Th in the studied Kamlial mudstone and sandstone are markedly lower than the corresponding values in the upper continental crust (UCC) and PAAS (Tables 1 and 4). Although there is some overlap, the average Ba concentration in the Kamlial samples is also considerably

Table 2. Whole-rock major element composition of the Kamlial sandstone from southwestern Kohat plateau, NW Pakistan, compared with the corresponding mean compositions of lithic arenite and K-feldspar-rich arenite. The numbers in parentheses show the average amounts in the Kamlial sandstone.

Oxides	Lithic arenite (Pettijohn et al., 1987)	K-feldspar-rich arenites (Pettijohn et al., 1987)	Kamlial Formation (this study)
SiO_2	66.1	66.2	46.9–63.4 (52.6)
Al_2O_3	8.1	10.2	6.1–23.3 (9.83)
Fe_2O_3	3.8	7.0 (T)	2.5–4.8 (3.7) (T)
FeO	1.4	-	-
MgO	2.4	4.5	0.9–3.5 (2.2)
CaO	6.2	2.0	7.5–20.4 (14.5)
Na_2O	0.9	1.8	0.5–1.4 (1.0)
K_2O	1.3	1.6	1.1–1.7 (1.3)
H_2O^+	3.6	-	-
H_2O^-	0.7	0.5	-
TiO_2	0.3	-	0.3–0.9 (0.7)
P_2O_5	0.1	-	(0.1)
MnO	0.1	0.2	0–0.2 (0.13)
CO_2	5.0	6.2?	-

Table 3. Oxide and element ratios in the Kamlial sandstone and mudstone samples from southwestern Kohat plateau, NW Pakistan. The letter in the sample numbers refers to locality: C for Chashmai anticline, A for Banda Assar syncline, and B for Bahadar Khel anticline.

Rock type	Sandstone											Mudstone				
Sample #	C-1	C-4	C-10	A-40	A-42	A-44	A-52	B-88	B-95	B-97	B-100	C-8	A-41	A-43	B-90	B-98
Na_2O/K_2O	0.67	0.34	0.44	0.88	0.97	1.03	0.99	0.65	0.66	0.80	0.74	0.52	0.48	0.58	0.27	0.66
K_2O/Al_2O_3	0.18	0.16	0.16	0.09	0.16	0.06	0.16	0.19	0.18	0.13	0.18	0.16	0.10	0.16	0.27	0.15
La/Y	2.28	2.11	1.04	1.70	1.11	1.28	2.17	2.37	1.32	1.77	2.41	1.80	2.07	1.80	1.32	1.75
U/Th	0.20	0.43	0.67	0.60	0.50	0.38	0.33	0.60	0.83	0.67	2.33	0.42	0.40	0.33	0.60	0.44
Rb/Sr	0.27	0.39	0.23	0.27	0.22	0.29	0.30	0.43	0.26	0.38	0.28	0.42	0.87	0.49	0.24	0.44
Auth. U	–0.67	0.67	2.00	1.33	1.00	0.33	0.00	1.33	3.00	2.00	12.00	1.00	0.67	0.00	2.67	1.00
V/Cr	0.31	0.18	0.67	0.14	0.20	0.29	0.49	0.28	0.33	0.16	0.20	0.88	0.80	1.05	1.13	0.25
Ni/Co	2.60	2.24	0.83	0.76	1.23	0.70	0.90	5.05	1.37	2.24	1.81	4.00	4.81	1.92	4.16	7.73
Cu/Zn	0.21	0.53	0.30	0.38	0.22	0.28	0.54	0.12	0.38	0.21	0.12	0.48	0.43	0.43	0.53	0.34
Ti/Zr	39.75	78.39	68.47	67.71	61.44	76.53	72.88	77.35	87.87	71.94	54.26	54.39	87.40	57.76	125.39	71.16
Cr/Ti	0.05	0.03	0.01	0.04	0.03	0.02	0.01	0.03	0.02	0.05	0.03	0.01	0.01	0.01	0.01	0.02
K/Rb	332	289	295	227	253	217	202	233	233	245	264	210	191	236	242	240
Cr/Ni	1.45	2.50	2.16	6.69	5.98	7.25	1.69	0.86	4.23	4.46	2.35	1.35	1.22	2.30	1.23	1.69
Cr/Th	31.85	41.91	14.27	49.91	25.52	26.66	10.40	36.72	29.19	64.95	32.69	7.85	11.78	6.12	9.62	32.24
Cr/Sc	11.52	24.36	6.69	22.73	13.18	19.47	4.09	15.52	9.12	32.47	11.51	7.72	9.14	3.22	5.17	19.79
Zr/Th	15.78	15.31	16.97	20.65	15.46	14.43	12.96	17.48	15.92	19.02	18.66	15.18	11.34	9.70	11.95	18.30
Zr/Sc	5.71	8.90	7.95	9.41	7.98	10.54	5.10	7.39	4.97	9.51	6.57	14.92	8.80	5.10	6.42	11.23

lower than that in UCC and PAAS (Table 4). On average, samples from the present study are slightly enriched in U relative to both UCC and PAAS (Tables 1 and 4). Compared to UCC and PAAS, all the studied sandstone and most mudstone samples contain low amounts of Cs, thus suggesting moderate chemical weathering (Tables 1 and 4) (Yan et al., 2007).

4.4.2. Weathering and sedimentary recycling

Uranium and thorium in sedimentary rocks are associated with several phases, such as clay minerals, feldspars, heavy minerals, phosphates, and organic matter (Ruffell and Worden, 2000). Whereas U is highly soluble even in neutral aqueous solutions, Th may dissolve in weak acids, such as humic acids (Pierini et al., 2002).

Sedimentary recycling under oxidizing conditions results in fractionation of Th and U during rock weathering; U^{+4} is readily oxidized to U^{+6}, which forms the highly soluble species uranyl ion, which can be removed from the system, whereas Th retains its oxidation state and remains relatively insoluble (McLennan and Taylor, 1980). As a consequence, the Th/U ratio increases due to successive cycles of weathering and redeposition and thus becomes a good marker of these processes. The Th/U ratio of the samples under investigation is less than the average value for UCC and PAAS (Tables 3 and 4), which suggests that these deposits are first-cycled. Further evidence of no sedimentary recycling can be seen from the Rb/Sr ratio (McLennan et al., 1993), which averages 0.3 for sandstone and 0.5 for mudstone from the study area (Tables 3 and 4). Similarly, the Zr/Sc ratio is commonly used as a measure of the degree of sedimentary recycling, which leads to the enrichment of the stable mineral zircon in the deposits (Nesbitt and Young, 1982). The Zr/Sc values of all the investigated Kamlial samples, except one mudstone, are lower significantly than both the UCC and PAAS values, indicating that a recycled sedimentary source was a minor component (Tables 3 and 4) (Roddaz et al., 2005).

4.4.3. Conditions during sediment deposition

U/Th ratios below 1.25 suggest deposition under oxic conditions, whereas values above 1.25 indicate suboxic and anoxic conditions (Nath et al., 1997). In the Arabian Sea, sediments below the oxygen minimum zone show

Table 4. Comparison of the average major element oxides (wt.%) and trace elements (ppm) of the Kamlial Formation (KF) with UCC and PAAS.

Specimen	UCC	PAAS	KF (avg.)
Major elements (wt.% oxides)			
SiO_2	65.92	62.80	41.96
Al_2O_3	15.20	18.90	12.76
Fe_2O_3	5.00	7.23	5.94
MgO	2.20	2.20	3.33
CaO	4.20	1.30	15.04
Na_2O	3.90	1.20	0.93
K_2O	3.37	3.70	1.89
TiO_2	0.50	1.00	1.04
P_2O_5	-	0.16	0.10
MnO	0.08	0.11	0.12
Trace elements (ppm)			
Sc	11	16	15
V	60	150	84
Cr	35	110	131
Co	10	23	18
Ni	20	55	88
Cu	25	50	28
Zn	71	85	62
Ga	-	20	11
Rb	112	160	86
Sr	350	200	201
Y	22	27	19
Zr	190	210	134
Nb	14	19	10
Cs	-	15	15
Ba	550	650	174
La	30	38	33
Ce	64	80	41
Nd	26	32	34
Sm	4	5	2
Yb	2	3	2
Hf	6	5	6
Pb	20	20	16
Trace elements (ppm)			
Th	11	15	10
U	3	3	4
Zr/Sc	17	13	9
Rb/Sr	0.32	0.80	0.43
U/Th	0.27	0.20	0.40
V/Cr	1.70	1.36	0.64
Cu/Zn	0.35	0.59	0.41
Ni/Co	2.00	2.39	4.89

high U/Th ratios (>1.25), whereas the sediments above the oxygen minimum zone exhibit low U/Th ratios (<1.25). Excluding one sample with an anomalous value, the low U/Th ratios in the studied samples suggest an oxic depositional environment for the Kamlial Formation (Table 3). Similarly, authigenic uranium content [= total U – Th/3] is also thought to be indicative of bottom water conditions in ancient sedimentary sequences (Wignall and Myers, 1988). Lower values of authigenic U (<5) represent oxic depositional conditions, while values above 5 are indicative of suboxic and anoxic conditions. The authigenic U contents are low in both the mudstone and sandstone samples under consideration (excluding one sandstone with anomalous value) (Table 3). Thus, the observed low U/Th ratio and low authigenic U content both show that the Kamlial sediments were deposited in an oxic environment.

The V/Cr ratio has also been used as an index of paleoxygenation in many studies (Bjorlykke, 1974; Dill et al., 1988). Vanadium may be bound to organic matter by the incorporation of V^{4+} into porphyrins, which is generally found in sediments deposited in reducing environments (Shaw et al., 1990). Chromium is mainly incorporated in the detrital fraction of sediments and it may substitute for Al in the structure of clays (Bjorlykke, 1974). V/Cr ratios of >2 indicate anoxic conditions, whereas values of <2 suggest more oxidizing conditions (Jones and Manning, 1994). The values and extent of variation in the V/Cr ratios in the mudstone and sandstone samples under discussion (Table 3) also imply that the Kamlial formation was deposited in an oxic environment. Dypvik (1984) used the Ni/Co ratio as a redox indicator. According to Jones and Manning (1994), Ni/Co ratios of <5 indicate oxic environments, whereas ratios of >5 suggest suboxic and anoxic environments. Sandstone from the current study shows Ni/Co ratios of <5, which suggests an oxygenated depositional environment, while the Ni/Co variation in mudstone (with one sample showing Ni/Co ratio of 7) indicates a suboxic environment (Table 3). Hallberg (1976) used Cu/Zn as a paleoredox parameter. According to him, high Cu/Zn ratios indicate reducing depositional conditions, while low Cu/Zn ratios suggest oxidizing conditions. The low Cu/Zn ratios for the studied Kamlial samples indicate that this mudstone-sandstone sequence was deposited under good oxidizing conditions (Table 3).

4.5. Paleoclimate of the source area

The average CIA values of sandstone and mudstone of the Kamlial Formation suggest moderate to slightly intense weathering at the source area. However, the high CIA values may also be due to the presence of abundant sedimentary rock fragments as occur in the associated sandstones rather than a result of severe weathering (Lee, 2002; Ullah et al., 2006). Similarly, the ICV values of the Kamlial mudstone

indicate somewhat moderate weathering in the source area. The presence of feldspar in the associated sandstones also supports this interpretation (Lee and Sheen, 1998; Ullah et al., 2006). Furthermore, the possibility of intensive chemical weathering in the Himalayas orogenic belt is highly unlikely, as it requires tectonic quiescence for a long period and higher temperature and humidity (Lasaga et al., 1994). Nonetheless, ample evidence exists indicating that the climate in northern Pakistan was warm, humid, subtropical to tropical, and influenced by monsoonal circulation throughout the time interval studied (Awasthi, 1982; West, 1984; Quade and Cerling, 1995). Paleoenvironmental reconstructions of the Siwalik sections in northern Pakistan indicate marked seasonality in paleosol formation, variation in rivers' discharge, and the existence of short-lived lakes (Zaleha, 1997). However, the presence of labile volcanic and metamorphic lithic fragments in these sequences suggests that petrography has not been drastically affected by weathering or diagenesis (Najman et al., 2003; Ullah et al., 2006).

In conclusion, the average CIA values of the Kamlial sandstone and mudstone from the southwestern part of the Kohat plateau suggest moderate to slightly intense weathering. However, the overall range of the ICV values and lower contents of Rb and Cs than UCC and PAAS of both the sandstone and mudstone indicate relatively moderate weathering. Furthermore, the Th/U ratio of the Kamlial Formation is lower than that of UCC and PAAS, which also shows that these sediments are first-cycle in origin. However, the Zr/Sc ratio suggests minor contribution from recycled sedimentary sources. The values of authigenic U, U/Th, V/Cr, Cu/Zn, and Ni/Co all suggest that the Kamlial sediments were deposited under oxidizing conditions.

Acknowledgments

The studies were performed at the National Center of Excellence in Geology, University of Peshawar, Pakistan, and were jointly financed by the Pakistan Atomic Energy Commission and the Higher Education Commission of Pakistan.

References

Ahmad S, Ali F, Ahmad I, Hamidullah S (2001). Geological map of the Kohat Plateau, NW Himalaya, NWFP. Peshawar, Pakistan: Geological Bulletin of the University of Peshawar.

Awasthi N (1982). Tertiary plant megafossils from the Himalaya - a review. Palaeobotanist 30: 25–267.

Bjorlykke K (1974). Geochemical and mineralogical influence of Ordovician island arcs on epicontinental clastic sedimentation: a study of Lower Palaeozoic sedimentation in the Oslo region, Norway. Sedimentology 21: 251–272.

Connor JJ (1990). Geochemical stratigraphy of the Yellowjacket Formation (Middle Proterozoic) in the area of the Idaho Cobalt Belt, Lemhi County, Idaho, with analytical contributions from Bartel AJ, Brandt E, Briggs PH, Danahey S, Fey D, Hatfield DB, Malcolm M, Merritt V, Riddle G, Roof S et al. USGS Open-File Report 90-0234: 1–30.

Cox R, Lowe DR, Cullers RL (1995). The influence of sediment recycling and basement composition on evolution of mudrock chemistry in the southwestern United States. Geochim Cosmochim Acta 59: 2919–2940.

Critelli S, Garzanti E (1994). Provenance of the Lower Tertiary Murree Redbeds (Hazara-Kashmir Syntaxis, Pakistan) and initial rising of the Himalayas. Sediment Geol 89: 265–284.

Cullers RL (2000). The geochemistry of shales, siltstones and sandstones of Pennsylvanian-Permian age, Colorado, USA: implications for provenance and metamorphic studies. Lithos 51: 181–203.

DeCelles PG, Gehrels GE, Quade J, Ojha TP, Kapp PA, Upreti BN (1998). Neogene foreland basin deposits, erosional unroofing and the kinematic history of the Himalayan fold-thrust belt, western Nepal. Geol Soc Am Bull 110: 2–21.

Dill H, Teshner M, Wehner H (1988). Petrography, inorganic and organic geochemistry of Lower Permian Carboniferous fan sequences (Brandschiefer Series) FRG. Constraints to their palaeogeography and assessment of their source rock potential. Chem Geol 67: 307–325.

Dypvik H (1984). Geochemical compositions and depositional conditions of Upper Jurassic and Lower Cretaceous Yorkshire clays, England. Geol Mag 121: 489–504.

Fedo CM, Nesbitt HW, Young GM (1995). Unraveling the effects of potassium metasomatism in sedimentary rocks and paleosols, with implications for paleoweathering conditions and provenance. Geology 23: 921–924.

Govindaraju K (1989). Compilation of working values and sample description of 272 geostandards. Geostandards Newsletter 13: 1–113.

Gu ZY, Lal D, Liu TS, Guo ZT, Southon J, Caffee MW (1997). Weathering histories of Chinese loess deposits based on uranium and thorium series nuclides and cosmogenic ^{10}Be. Geochim Cosmochim Acta 61: 5221–5231.

Hallberg RO (1976). A geochemical method for investigation of paleoredox conditions in sediments. Ambio Spec Rep 4: 139–147.

Herron MM (1988). Geochemical classification of terrigenous sands and shales from core or log data. J Sediment Pet 58: 820–829.

Hodges KV (2000). Tectonics of the Himalaya and southern Tibet from two perspectives. Geol Soc Am Bull 112: 324–350.

Jones B, Manning DC (1994). Comparison of geochemical indices used for the interpretation of palaeoredox conditions in Ancient mudstones. Chem Geol 111: 111–129.

Kadri IB (1995). Petroleum Geology of Pakistan. Lahore, Pakistan: Ferozsons.

Kazmi AH, Rana RA (1982). Tectonic map of Pakistan: scale 1:2000000. Quetta, Pakistan: Geological Survey of Pakistan.

Kumar R, Ghosh SK, Sangode SJ (2003). Mio-Pliocene sedimentation history in the northwestern part of the Himalayan foreland basin, India. Current Sci 84: 1006–1113.

Lasaga AC, Soler JM, Ganor J, Burch TE, Nagy KL (1994). Chemical weathering rate laws and global geochemical cycles. Geochim Cosmochim Acta 58: 2361–2386.

Lee YI (2002). Provenance derived from the geochemistry of Late Paleozoic-Early Mesozoic mudrocks of the Pyeongan supergroup, Korea. Sediment Geol 149: 219–235.

Lee YI, Ko HK (1997). Illite crystallinity and fluid inclusion analysis across a Paleozoic disconformity in central Korea. Clays Clay Min 45: 147–157.

Lee YI, Sheen DH (1998). Detrital modes of the Pyeongan Supergroup (Late Carboniferous-Early Triassic) sandstones in the Samcheog coalfield, Korea: Implication for provenance and tectonic setting. Sediment Geol 119: 219–238.

Lindsey DA, Tysdal RG, Taggart JE Jr (2003). Chemical composition and provenance of the Mesoproterozoic Big Creek, Apple Creek, and Gunsight Formations, Lemhi Group, Central Idaho. In: Russell G, Tysdal RG, Lindsey DA, Taggart JE Jr, editors. Correlation, Sedimentology, Structural Setting, Chemical Composition, and Provenance of Selected Formations in Mesoproterozoic Lemhi Group, Central Idaho. Washington, DC, USA: USGS Professional Paper 1668-B.

McLennan SM, Hemming S, McDaniel DK, Hanson GN (1993). Geochemical approaches to sedimentation, provenance and tectonics. In: Johnsson MJ, Basu A, editors. Processes Controlling the Composition of Clastic Sediments. Boulder, CO, USA: Geological Society of America Special Paper 284, pp. 21–40.

McLennan SM, Taylor SR (1980). Th and U in sedimentary rocks: crustal evolution and sedimentary recycling. Nature 285: 621–624.

Meigs AJ, Burbank DW, Beck RA (1995). Middle-late Miocene (>10 Ma) formation of the Main Boundary thrust in the western Himalaya. Geology 23: 423–426.

Meissner CR, Master JM, Rashid MA, Hussain M (1974). Stratigraphy of the Kohat Quadrangle, Pakistan. USGS Prof Pap 716-D: 1–30.

Metcalfe RP (1993). Pressure, temperature and time constraints on metamorphism across the Main Central Thrust zone and High Himalayan slab in the Garhwal Himalaya. In: Treloar PJ, Searle MP, editors. Himalayan Tectonics. London, UK: Geological Society of London Special Publication 74, pp. 485–509.

Najman Y (2006). The detrital record of orogenesis: a review of approaches and techniques used in the Himalayan sedimentary basins. Earth Sci Rev 74: 1–72.

Najman Y, Garzanti E, Pringle M, Bickle M, Stix J, Khan I (2003). Early-Middle Miocene paleodrainage and tectonics in the Pakistan Himalaya. Geol Soc Am Bull 115: 1265–1277.

Nath BN, Bau M, Ramalingeswara Rao B, Rao CM (1997). Trace and rare earth elemental variation in Arabian Sea sediments through a transect across the oxygen minimum zone. Geochim Cosmochim Acta 61: 2375–2388.

Nesbitt HW, Markovics G, Price RC (1980). Chemical processes affecting alkalis and alkaline earths during continental weathering. Geochim Cosmochim Acta 44: 1659–1666.

Nesbitt HW, Young GM (1982). Early Proterozoic climates and plate motions inferred from major element chemistry of lutites. Nature 299: 715–717.

Pettijohn FJ, Potter PE, Siever R (1987). Sand and Sandstone. 2nd ed. New York, NY, USA: Springer.

Pierini C, Mizusaki AMP, Scherer CMS, Alves DB (2002). Integrated stratigraphic and geochemical study of the Santa Maria and Caturrita formations (Triassic of the Parana Basin), southern Brazil. J South Am Earth Sci 15: 669–681.

Potter PE, Maynard JB, Pryor WA (1980). Sedimentology of Shale. Berlin, Germany: Springer-Verlag.

Quade J, Cerling TE (1995). Expansion of C4 grasses in the Late Miocene of Northern Pakistan: evidence from stable isotopes in paleosols. Palaeo Palaeo Palaeo 115: 91–116.

Raiverman V (2002). Foreland Sedimentation in Himalayan Tectonic Region: A Relook at the Orogenic Process. Dehradun, India: Bishen Singh Mahendra Pal Singh.

Roddaz M, Viers J, Brusset S, Baby P, Herail G (2005). Sediment provenances and drainage evolution of the Neogene Amazonian foreland basin. Earth Planetary Sci Lett 239: 57–78.

Ruffell A, Worden R (2000). Palaeoclimate analysis using spectral gamma-ray data from the Aptian (Cretaceous) of southern England and southern France. Palaeo Palaeo Palaeo 155: 265–283.

Searle MP, Corfield RI, Stephenson B, McCarron J (1997). Structure of the north Indian continental margin in the Ladakh-Zanskar Himalayas: Implications for the timing of obduction of the Spontang ophiolite, India-Asia collision and deformation events in the Himalaya. Geol Mag 134: 297–316.

Seeber L, Armbruster JG, Quittmeyer RC (1981). Seismicity and continental subduction in the Himalayan arc. In: AGU Geodynamics Series 5, Washington, DC, USA, pp. 259–279.

Seeber L, Gornitz V (1983). River profiles along the Himalayan arc as indicators of active tectonics. Tectonophysics 92: 335–367.

Shah SMI (2009). Stratigraphy of Pakistan. Quetta, Pakistan: Geological Survey of Pakistan Memoir 22.

Shaw TJ, Geiskes JM, Jahnke RA (1990). Early diagenesis in differing depositional environments: the response of transition metals in pore water. Geochim Cosmochim Acta 54: 1233–1246.

Ullah K, Arif M, Shah MT (2006). Petrography of sandstones from the Kamlial and Chinji formations, southwestern Kohat plateau, NW Pakistan: implications for source lithology and paleoclimate. J Himalayan Earth Sci 39: 1–13.

Valdiya SK (1992). The Main Boundary Thrust zone of Himalaya, India. Annal Tectonicae 6: 54–84.

Vance D, Harris N (1999). Timing of prograde metamorphism in the Zanskar Himalaya. Geology 27: 395–398.

West RM (1984). Siwalik faunas from Nepal: palaeoecologic and palaeoclimatic implications. In: Whyte RO, editor. The Evolution of the East Asian Environment. Hong Kong: Centre for Asian Studies, University of Hong Kong, pp. 724–744.

Wignall PB, Myers KJ (1988). Interpreting the benthic oxygen levels in mudrocks, a new approach. Geology 16: 452–455.

Yan Y, Xia B, Lin G, Cui X, Hu X, Yan P, Zhang F (2007). Geochemistry of the sedimentary rocks from the Nanxiong Basin, South China and implications for provenance, palaeoenvironment and palaeoclimate at the K/T boundary. Sediment Geol 197: 127–140.

Yin A (2006). Cenozoic tectonic evolution of the Himalayan orogen as constrained by along-strike variation of structural geometry, exhumation history, and foreland sedimentation. Earth Sci Rev 76: 1–131.

Zaleha MJ (1997). Intra- and extra-basinal controls on fluvial deposition in the Miocene Indo-Gangetic foreland basin, northern Pakistan. Sedimentology 44: 369–390.